

ERDC/CRREL TR-12-7

Cold Regions Research
and Engineering Laboratory



**US Army Corps
of Engineers®**
Engineer Research and
Development Center

Effects of Support Structure Porosity on the Drift Accumulation Surrounding an Elevated Building

Arnold Song and Robert Haehnel

September 2012



Effects of Support Structure Porosity on the Drift Accumulation Surrounding an Elevated Building

Arnold Song and Robert Haehnel

*Cold regions Research and Engineering Laboratory
U.S. Army Engineer Research and Development Center
72 Lyme Road
Hanover, NH 03755*

Final report

Approved for public release; distribution is unlimited.

Prepared for National Science Foundation
Office of Polar Programs, AIL
Arlington, VA

Abstract:

This study focuses on the effects of elevated building substructure porosity on the accumulation of drifting snow. We conducted wind tunnel experiments of the snowdrift accumulation and numerical simulations to determine the flow field around a prototypical elevated building (based on the Martin A. Pomerantz Observatory or MAPO) with varying substructure porosity. We found that the total drift volume accumulated decreases as the substructure porosity increases (i.e., the substructure has less clutter). Furthermore, substructure porosity influenced the proportion of the drift deposited upwind or downwind of the structure, with a more porous substructure depositing most of the drift upwind of the structure; for low substructure porosity, most of the drift is deposited in the lee of the structure. Numerical simulations revealed that, for low substructure porosity a separation bubble can form upwind of the building that appears to direct particles over the upwind region of subcritical shear stress and suppress formation of the upwind snowdrift. Porosity and the presence of ground-based clutter also affected the rate of drift encroachment. The results of this study suggest that applying care in the design of the substructure could prolong the life of a building by 2 or more years.

DISCLAIMER: The contents of this report are not to be used for advertising, publication, or promotional purposes. Citation of trade names does not constitute an official endorsement or approval of the use of such commercial products. All product names and trademarks cited are the property of their respective owners. The findings of this report are not to be construed as an official Department of the Army position unless so designated by other authorized documents.

DESTROY THIS REPORT WHEN NO LONGER NEEDED. DO NOT RETURN IT TO THE ORIGINATOR.

Table of Contents

| | |
|---|-----------|
| Abstract | ii |
| List of Figures and Tables | iv |
| Preface | v |
| Executive Summary | vi |
| 1 Introduction | 1 |
| 2 Physical Modeling of Snowdrifting | 4 |
| 3 Validation of time scaling | 7 |
| 3.1 Modeling approach..... | 9 |
| 3.2 Model results | 10 |
| 4 Prototype Elevated Building | 13 |
| 4.1 Experiment description | 13 |
| 4.2 Total accumulated drift volume | 14 |
| 4.3 Upwind drift development..... | 15 |
| 4.4 Drift encroachment | 16 |
| 4.5 Downwind drift development | 17 |
| 5 CFD experiments | 23 |
| 5.1 Approach | 23 |
| 5.2 Results | 24 |
| 6 Concluding remarks | 29 |
| 6.1 Significant findings..... | 29 |
| 6.2 Suggestions for future work..... | 31 |
| 6.2.1 Continuation of the numerical snowdrift deposition model development..... | 31 |
| 6.2.2 Control of drifting snow on garage shop entrance..... | 31 |
| References | 33 |
| Report Documentation Page | |

List of Figures and Tables

Figures

| | |
|--|----|
| Figure 1. Drift survey at the end of 2009 winter season. | 1 |
| Figure 2. Experimental set up for the wind tunnel experiments..... | 5 |
| Figure 3. Met data from the 2007 winter season, Amundsen-Scott South Pole Station. | 8 |
| Figure 4. Wind tunnel drift profile illustrating measurement region of interest..... | 9 |
| Figure 5. Comparison of field and model upwind drift volumes..... | 10 |
| Figure 6. MAPO prototype building with baseline support structure..... | 13 |
| Figure 7. Total accumulated drift deposited around the simulated MAPO building configurations evaluated. | 14 |
| Figure 8. Upwind drift development as a function of elevated platform configuration. | 15 |
| Figure 9. Drift encroachment..... | 16 |
| Figure 10. Comparison of downwind drift volumes with experiment done by Kwok et al. (1993). | 18 |
| Figure11. Comparison of the concentration of particles carried by the wind between the field condition and that estimated for the model cases. | 20 |
| Figure 12. Schematic of CFD configuration..... | 23 |
| Figure 13. Wall shear stress magnitude. | 25 |
| Figure 14. Building centerline velocity magnitude fields..... | 28 |

Tables

| | |
|---|---|
| Table 1. Estimation of seasonal snow transport for Amundsen-Scott South Pole Station. | 8 |
|---|---|

Preface

This study was conducted for the National Science Foundation, Office of Polar Programs, AIL.

The work was performed by Arnold Song and Robert Haehnel (Terrestrial and Cryospheric Sciences Branch, Janet Hardy, Chief), U.S. Army Engineer Research and Development Center–Cold Regions Research and Engineering Laboratory (ERDC-CRREL). At the time of publication, Dr. Justin Berman was Chief of the Research and Engineering Division. The Deputy Director of ERDC-CRREL was Dr. Lance Hansen and the Director was Dr. Robert Davis.

The authors thank Jesse Stanley and Troy Arnold for their assistance in conducting the wind tunnel experiments. The scale wind tunnel models were fabricated by Russ Kelly. They sincerely thank George Blaisdell at NSF/OPP-AIL for his support of this snowdrift study.

At the time this report was prepared, COL Kevin J. Wilson was the Commander and Executive Director of ERDC, and Dr. Jeffery P. Holland was the Director.

Executive Summary

In austere environments, such as Antarctica, snowdrift accumulation around buildings not only presents safety hazards to personnel, but also can significantly shorten the service life of the building. Elevated structures are a common and effective design strategy to combat drift accumulation in proximity to buildings. However, the foundation structure or substructure that is used to elevate the building above grade may impede or choke off the flow thereby increasing the drift accumulation and reducing the effectiveness of elevating the building. This study focuses on the effects of building substructure porosity on the accumulation of drifting snow.

Initial tests compared the snowdrift evolution between a scale wind tunnel model of the Amundsen-Scott South Pole Station and field surveys. We observed good agreement between the wind tunnel and field data upon applying the time scaling proposed by Lever and Haehnel (1995).

Using this time scaling, we conducted wind tunnel experiments of the snowdrift accumulation and numerical simulations to determine the flow field around a prototypical elevated building (based on the Martin A. Pomerantz Observatory or MAPO at South Pole Station) with varying substructure porosity. We found that the total drift volume decreases as the substructure porosity increases (i.e., the substructure has less clutter that can impede flow under the structure). This total drift volume was divided between drifts formed upwind and downwind of the building. For the low porosity case (more substructure clutter), the drift volume was concentrated downwind and, as the building porosity increases, the drift volume is concentrated more heavily upwind of the building.

Numerical simulations of the elevated building prototype were used to take a closer look at how substructure porosity affects the flow field around the building. Regions of wall shear stress that fall below the threshold shear stress required for particle transport were identified and considered to be areas where drifts would likely form. Yet, we identified other flow structures that influence drift accumulation as well. For example, we observed that, at a low substructure porosity, when the flow beneath the building is heavily choked, a separation bubble forms upwind of the building. This separation bubble acts as a physical bump and directs

particles over the upwind region of subcritical shear stress and impedes the growth of the upwind snowdrift. This flow structure may explain the trend we observed in the wind tunnel experiments, where the upwind drift volumes were lower for the lower porosity substructures, forcing the drift to preferentially form downwind in this case.

Some features under the building, such as the support structure, can promote drifting close to the building and cause the drift to rapidly encroach on the building. This is a potentially dangerous drifting behavior that may also lead to a shorter building service lifespan. We observed that a substructure composed of a dense matrix of support posts increased the rate that the drift approached the front of the building by 1.5 times. But, porosity was not the only factor affecting drift encroachment. The support structure may have span-wise cross members. These will serve as nucleation points for drift formation and allow the drift to form much closer to the building than would occur for a substructure clear of these features. Careful thought during the design phase needs to be given to avoiding such structural features that promote drifting. The results of this study suggest that applying such care in the design could prolong the life of a building having the same configuration as the MAPO by 2 or more years.

1 Introduction

Despite the small amount of background snow accumulation of roughly 24.1 cm (8.4 cm of water equivalent) annually at the South Pole (Mosley-Thompson et al. 1999), the drift accumulations near and around buildings can be quite large. Surveys of the snow drifts around the Amundsen-Scott South Pole Station document upwind drifts accumulating to more than 1.4 m high for a winter season, with a total peak drift height of approximately 4 m above the grade beam level (Skoog 2009). These drifts contain large volumes of snow; for example, the drift upwind of the elevated South Pole station, shown in Figure 1, had a seasonal volume accumulation of nearly 10,000 m³ in FY09. The significant size of these drifts can lead to safety issues by blocking building access points, contributing to increased snow loads, or completely burying a building.

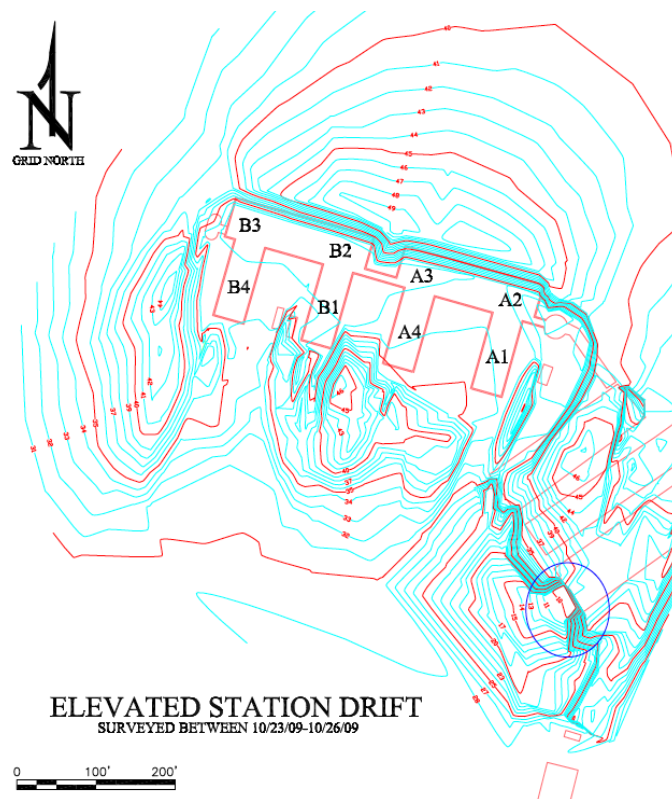


Figure 1. Drift survey at the end of 2009 winter season. Elevations and distances in feet (0.3048 ft = 1 m). (Drift survey performed and drawing generated by Kurtis Skoog, Raytheon Polar Services Company, Centennial, CO.)

Snowdrift control and maintenance require many man-hours and use of heavy equipment, not only incurring significant cost but also tying up valuable equipment time; therefore, an effort has been made to incorporate snow control features into the building designs for areas that experience large amounts of drifting snow. A highly effective and widely used design strategy employed to control drifting around buildings in regions such as Antarctica is to elevate the buildings. By lifting these aerodynamically bluff bodies above the ground, a Venturi effect is created whereby the fluid accelerates as it is squeezed between the building and the ground. This fast moving flow keeps the area near and under the building swept clear of snow. In addition, chamfered edges are used on the buildings to help to streamline the structure, which reduces the size of the wake region and subsequently downwind drift size (Kwok et al. 1993).

Previous studies have looked at how a building's elevated height, orientation to the oncoming flow, edge geometry, etc. (Kwok et al. 1993; Kim et al. 1990), contribute to the drift development around it. Ideally, the area beneath an elevated building would be completely clear of any "clutter," e.g., stairways, support columns, miscellaneous equipment, etc., which will impede the flow under the building and diminish the Venturi effect. But, in practice, keeping the area between the building and the ground clutter-free can be difficult. The focus of this study is to understand how the porosity within the building support structure (substructure) affects the drift accumulation near the building, which ultimately determines the design life of the building, i.e. when the building either becomes buried or needs to be moved or further elevated.

In this study we used a combination of wind tunnel and numerical modeling to understand the effects of substructure porosity on drift evolution. A brief outline of this report follows.

- Section 2: The methods used in this study for wind tunnel modeling of drifting snow are described.
- Section 3: An important part of this effort is to determine the rate of drift development around the buildings, so in this section we validated the methodology proposed by Lever and Haehnel (1995) and Anno (1984) for scaling time between model and prototype using field data of drift evolution obtained around the Amundsen-Scott (A-S) South Pole Station from 2007 to 2009. These data are compared to model results obtained in the CRREL wind tunnel facility.

- Section 4: Using the validated time scaling method, we applied this scaling to determine the drift development rates for a simplified model of the Martin A. Pomerantz Observatory (MAPO) building to study how the substructure porosity affects snow drift formation.
- Section 5: We present Computational Fluid Dynamics (CFD) simulations of the MAPO prototype building that examined the effect of substructure porosity on the flow around the building and the flow condition that led to snow drift development.
- Section 6: Conclusions and recommendations.

2 Physical Modeling of Snowdrifting

Wind tunnel tests were performed in the CRREL wind tunnel with scale models of the Amundsen-Scott (A-S) South Pole Station (1:250 scale) and a simplified version of the MAPO building (1:30 scale) using fine, spherical glass beads (mean diameter 130 μm) as the snow simulant. The horizontal dimension of the A-S station was the limiting factor in determining the scale of the model; this dimension was held to $\frac{1}{4}$ of the tunnel width to keep the boundary layer on the walls of the wind tunnel from influencing the flow around the model. The height of the MAPO model was the limiting factor in setting the scale of that model, as the traversing gear used for measuring the drift profiles needed to be able to pass over the model unimpeded.

Another factor that influences model size is solid blockage, or the decrease in the wind tunnel's open cross-sectional area attributable to the model's presence. To satisfy conservation of mass, the flow accelerates as it moves past and around the model, such that $U_M = (1 + \varepsilon_B)U_T$, where U_T is the average velocity in the tunnel at the location where the model is to be placed and U_M is the elevated velocity in the vicinity of the model when it is placed in the tunnel at that location. This local increase of the velocity is quantified by a blockage factor, ε_B , defined by Thom (1943):

$$\varepsilon_B = \frac{KV_M}{A_T^{3/2}} \quad (1)$$

where

$K \approx 0.96$ for bluff bodies

V_M = volume of the model

A_T = cross-sectional area of the wind tunnel test section.

The goal is to keep U_M/U_T very close to unity by minimizing ε_B . A generally accepted rule of thumb is to keep the localized velocity increase attributable to the model under 10% of the unobstructed freestream velocity. We were well under this criterion, with the largest model in this study having a volume of 0.04 m^3 and the cross-section of the wind tunnel being 3.0 m^2 $\varepsilon_B \leq 0.008$ for all of our model runs. This translates to less than a 1%

change in the flow velocity being introduced by blockage caused by the models tested in this study.

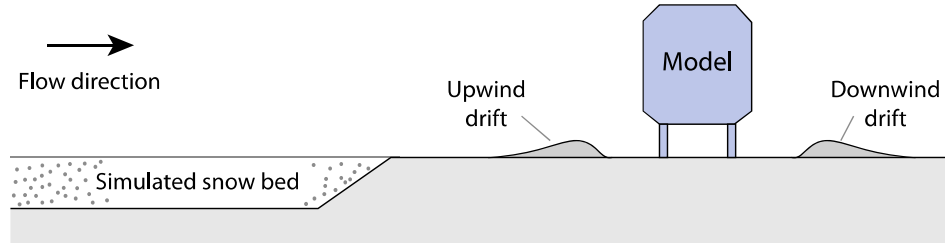


Figure 2. Experimental set up for the wind tunnel experiments (not to scale).

The experiments were conducted as follows. The model buildings were placed downstream of a large bed of the glass beads, which served as the source of drifting material as depicted in Figure 2. During the course of the experiment, the wind would pick up particles from the upstream reservoir and carry the simulated snow particles to the model. Some of the particles were deposited in the wake regions surrounding the models, and others were transported beyond the model and captured in sediment traps. The wind tunnel was run at a constant speed for a specified time to ensure that the transport rate was nearly constant throughout the experiment. Owing to the limited amount of material that could be stored in the particle reservoir, each experiment was run as a series of stages where the particle bed was replenished after a set period. The transported material was then weighed before being replaced in the particle reservoir. For each stage, 3-dimensional drift profiles were acquired using a laser surface profilometer, where each stage's profile would provide a snapshot of the drift evolution as a function of the material transported.

We followed the approach of Lever and Haehnel (1995) to scale time between the model and prototype using the non-dimensional mass transport parameter as proposed by Anno (1984):

$$T^* = \frac{qt}{\rho_b H^2} \quad (2)$$

where the mass transport per unit width, qt , is scaled by the particle bulk density, ρ_b , and a characteristic area, H^2 . For the wind tunnel experiments and field data, we used the height of the buildings (excluding the substructure height) as the value for H . We used this scaling of the snow transport,

T^* , as non-dimensional time that allowed us to correlate the drift evolution in the field with the drift behavior observed at the model scale.

We must acknowledge the limitations on direct correlation between the drifting experiments conducted in the wind tunnel and the drift formation observed in the field. There are several sources of distortion in the wind tunnel experiments, but we focus on the two most influential sources of model distortion: 1) Froude distortion and 2) particle cohesion.

The Froude number is a dimensionless parameter that compares the inertial effects to gravitational effects and is defined as

$$\text{Fr} = \frac{U^2}{gL} \quad (3)$$

where

- U = freestream velocity
- g = gravitational acceleration
- L = characteristic length.

The Froude number for the wind tunnel experiments, $\text{Fr} = 13.8$, is significantly higher than field values, $\text{Fr} = 0.070$, indicating the particle trajectories in the wind tunnel are proportionally much longer than those seen by snow particles in the field. However, Lever and Haehnel (1995) suggested that Froude distortion will not have a significant effect on overall drift behavior as long as particle trajectories are much shorter than drift lengths. Keeping wind velocities near transport threshold velocities will typically satisfy this latter requirement, even though Froude distortion cannot be eliminated.

With respect to model distortion caused by particle cohesion, the transport characteristics of freshly fallen snow can be very different from old snow because of snow metamorphism and sintering. The sintering of adjacent snow grains can provide erosion resistance in flow conditions that would otherwise cause cohesionless particles to blow away. The glass beads used as a proxy for snow in the wind tunnel experiments are essentially cohesionless and certainly do not sinter over time. Therefore, we expected the drift growth rates observed in the wind tunnel experiments to lag behind the field measurements owing to the effects of Froude distortion and lack of particle cohesion.

3 Validation of time scaling

First, we wanted to verify the drift volume scaling of Lever and Haehnel (1995) by comparing the drift evolution measured in the field at the A-S South Pole station and a 1:250 scale model placed in the CRREL wind tunnel. The mass transport, qt , for the wind tunnel experiments was measured by weighing the transported particles for each experiment stage, but direct field measurements of the snow mass transport for the Amundsen-Scott Station location are not available. For this, we relied on the empirical expression obtained by Tabler (1991), a best-fit to the Antarctic field measurements of Budd et al. (1966), to determine the horizontal snow mass transport as a function of the wind speed measured at 10 m above the snow surface, U_{10} (m/s), as follows:

$$q_{0-5} = U_{10}^{3.8} / (233,846) \quad (4)$$

In this expression, q_{0-5} (kg/m·s), is the integrated snow mass flux per unit width from the snow surface to a height of 5 m. We then calculated the value of T^* for a specific winter season by integrating Tabler's expression, using the available meteorological (or met) data for the A-S station. The met data used to estimate snow transport for the 2007 season are shown in Figure 3. Three seasons (2007–2009) of field drift surveys and met data were used in this comparison of model and field drift development. The estimated transport for these three seasons is summarized in Table 1.

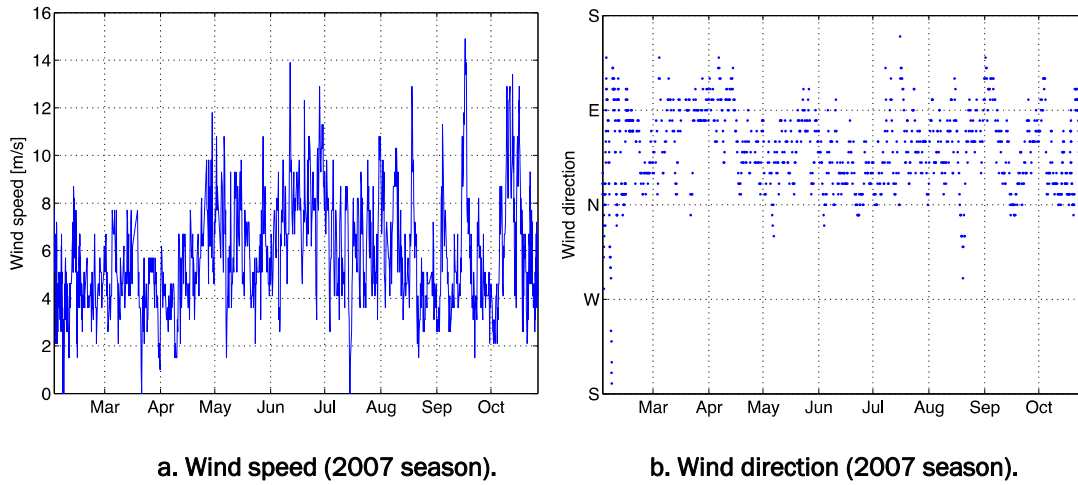


Figure 3. Met data from the 2007 winter season, Amundsen-Scott South Pole Station.

Table 1. Estimation of seasonal snow transport for Amundsen-Scott South Pole Station. The horizontal snow transport for each season was estimated from wind velocities (met data from the 2007 winter season are shown as an example in Fig. 3) using Tabler’s empirical expression.

| Season | Estimated transport, Q [kg/m] | Non-dimensional transport, T^* |
|---------|---------------------------------|----------------------------------|
| 2007 | 1.56×10^5 | 4.7 |
| 2008 | 1.04×10^5 | 3.2 |
| 2009 | 1.80×10^5 | 5.3 |
| Average | 1.47×10^5 | 4.4 |

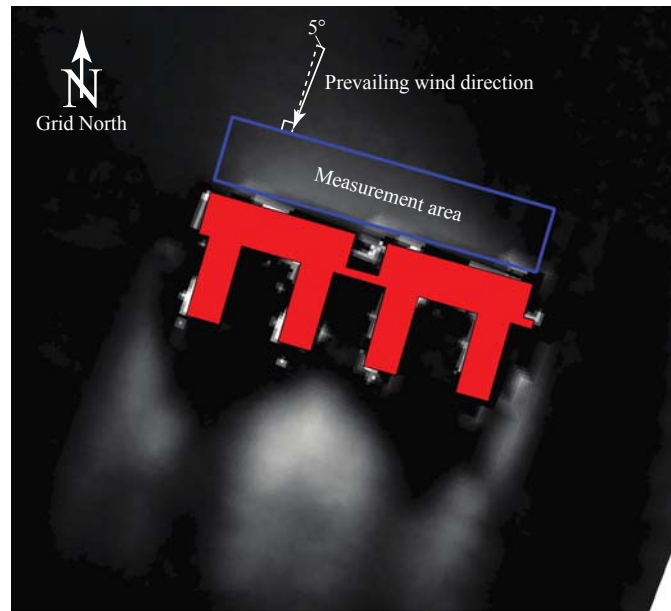


Figure 4. Wind tunnel drift profile illustrating measurement region of interest. The shading from black to white indicates the relative drift height, with black being zero accumulated drift, and white being the maximum measured height.

3.1 Modeling approach

The Amundsen-Scott Station is oriented so that the front of the station faces 16° east from grid north, while the prevailing winds blow from 21° east of north. To account for this, the wind tunnel model was rotated clockwise (viewed from the top) so that the front of the model was skewed 5° from perpendicular with respect to the oncoming flow (Fig. 4). All model runs were conducted at a constant wind speed, $U = 5.0$ m/s ($U/U_t = 2.8$, where U_t is the threshold velocity for particle transport). This wind speed was measured at a fixed elevation of 50 cm above the bed in the wind tunnel.

Having established a method for comparing drift transport between model and prototype, we now needed a way to compare the volumes of deposited drift. Surveys of the initial groomed berm were taken at the beginning of 2007 and 2008 and served as initial conditions for estimating the volume of snow that accumulates each winter. However, these surveys do not include the regions to the sides and downwind of the station, making quantitative comparisons between the model and field data in these areas difficult. Therefore, we focused on the upwind drift development for comparing model and prototype and validating the time scaling.

The blue box in Figure 4 delineates the region that we used for comparison of drift volumes between the model and field data. The rectangular measurement area spans the station's width, is 23 m long, and is offset 4.5 m upwind from the front of the station. The extent of the "sampling box" was restricted in the upwind direction to eliminate discrepancies between laboratory and field definitions of the drift toe line. Drift volume and cross-sectional area calculations were performed within the boundaries of this region for the field surveys as well as the wind tunnel experiments.

3.2 Model results

At the start of the 2007 and 2008 seasons, the snow accumulated in the upwind drift from the previous winter at Amundsen-Scott Station was partially removed and the snow that remained was shaped into a berm. For comparison with the wind tunnel model cases, we assumed that this groomed state was the initial condition for the drift evolution, i.e., $T^* = 0$. Therefore, the volume reported for the field case and plotted in Figure 5 is the snow volume that accumulated between the survey taken at the end of the summer season (beginning of February) and a subsequent survey taken soon after station open (beginning of November). In 2009, the upwind drift was not groomed into a smaller berm as in previous years; therefore, the upwind drift surveyed at the end of 2009 includes the previous season's accumulated volume as well.

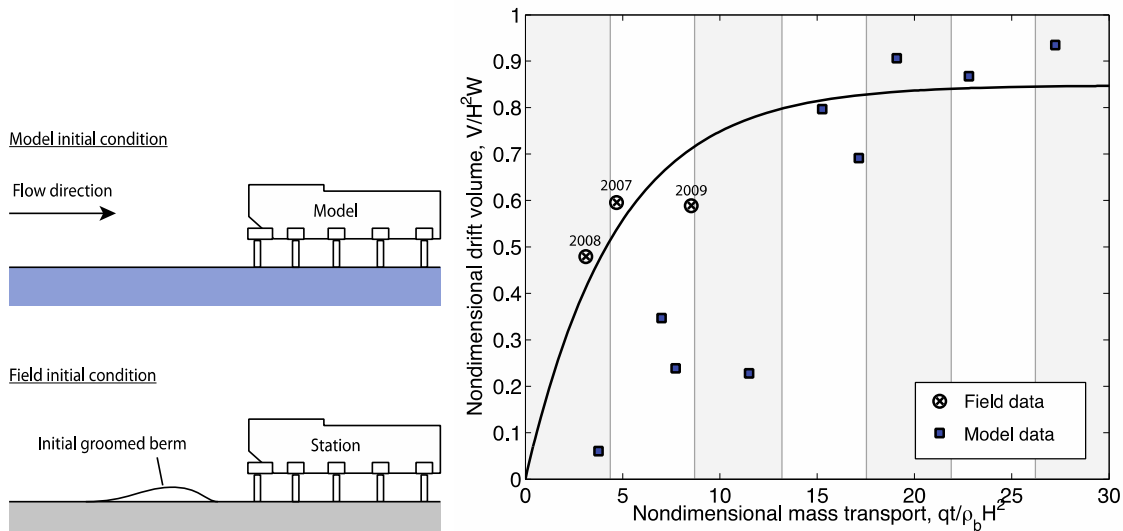


Figure 5. Comparison of field and model upwind drift volumes. The alternate gray and white shading indicates an elapsed time of about 1 year in the field.

To compare the drift behavior among the model and field cases, we used the following model expression:

$$V^* = \frac{V}{H^2W} = \alpha(1 - e^{\beta t^*}) \quad (5)$$

where $\alpha = 0.85$ and $\beta = 0.2$ are the nondimensional saturation drift volume and the decay time constant, respectively, which are determined by a least squares fit to the wind tunnel data. We chose the form of eq (5) to describe the behavior observed in the wind tunnel test data: a rapid initial drift development rate followed by a slowdown in growth as the drift volume asymptotically approached equilibrium. We assumed that the equilibrium drift volume, α , was the same for both the model and field data because the cases should approach similar equilibrium states, independent of the initial topography. Note that the reported value of the equilibrium drift volume, α , applies only to the drift volume that lies within the interrogation region and not the upwind drift in its entirety.

In Figure 5, we found relatively good agreement between the field and the wind tunnel model drift accumulation. The model accumulation did lag the field data initially, which we attributed to the model distortion described previously, namely Froude distortion and lack of particle cohesion. The comparison of the field data with the wind tunnel model measurements demonstrated that the method for scaling time outlined by Lever and Haehnel (1995) is adequate and can be applied to other geometries. This methodology was used in analysis of the data obtained in for the MAPO building experiments (Section 4).

It is interesting to note that, though the model seems the lag the field case initially, comparison of the model and prototype results suggested that, after an initial rapid growth of the upwind drift that spanned one–two seasons, the growth rate declined dramatically as the drift asymptotically approached the “equilibrium” volume.

It is difficult to talk of a true equilibrium condition at the South Pole as there is a net annual accumulation of approximately 24 cm, which causes the terrain to slowly rise around any fixed buildings. The Venturi effect caused by the reduced cross section beneath an elevated structure will help reduce snow accumulation under the building for a time. However, regular jacking of the elevated structure is required to prevent eventual inundation

from the combined effects of drifting and accumulated rise of the surrounding terrain.

Our findings suggest that the time for the drift to reach a quasi-equilibrium height is on the order of 5–6 years, and consideration for jacking the building should be on a similar time scale (e.g., 5 to 10 years) to stay ahead of the rising terrain.

The equilibrium volume for the upwind drift would likely be reached in 5–6 years of operation if the upwind drift were left untouched with no annual removal or re-shaping of the upwind drift. The approximate height of the equilibrium drift would be expected to be on the order of 4 to 5 m.

4 Prototype Elevated Building

4.1 Experiment description



Figure 6. MAPO prototype building with baseline support structure.

We also conducted wind tunnel drifting experiments on a 1:30 scale prototype that was based on the MAPO, which is a rectangular prism with chamfered edges (Fig. 6). As discussed previously, the aim of this study was to understand how clutter or blockage below the structure would influence the drift growth rate and deposition patterns. Three elevated building support configurations were tested in the wind tunnel: 1) a baseline configuration composed of truss work modeled after the current MAPO support structure (as shown in Fig. 6), 2) a high porosity case with support posts placed at each of the four corners at the bottom of the building, and 3) a low porosity case with a tightly packed array of posts below the building (0.6-cm-diameter posts spaced 3.3 cm apart center-to-center at model scale; at prototype scale, the posts are 19.1 cm diameter, with a center-to-center spacing of 1.00 m). For all the cases considered, the model was oriented so that the longer building dimension was perpendicular to the oncoming flow. As with the South Pole station experiments, the wind speed was set at $U = 5.0$ m/s and a nondimensional mass transport, T^* , served as the scale for time. For the drift volume, we used the scaling similar to that of Kwok et al. (1993) where the drift volume is normalized by the building volume:

$$V^* = V_{drift} / V_{building} \quad (6)$$

4.2 Total accumulated drift volume

In Figure 7, we compare the measured volume of the evolving drifts around the model buildings. The accumulated volume (sum of the drift volumes deposited upwind and downwind of the building) was the lowest when the porosity of the substructure was very high (green line). It is interesting to note that the baseline configuration's total drift volume (blue line) was nearly the same as the low porosity case (red line) at $T^* \approx 7$, despite significantly slower growth of the baseline case for times before this point. Despite the relatively open substructure of the baseline case, compared to the dense substructure of the low porosity case, the long-time drift volumes are similar. This seems to suggest that even small amounts of “clutter” can substantially increase drift volume and may reduce effective building life. Based on the wind tunnel results (Fig. 7), it appears that the time it will take to reach the equilibrium drift geometry is about 2 years.

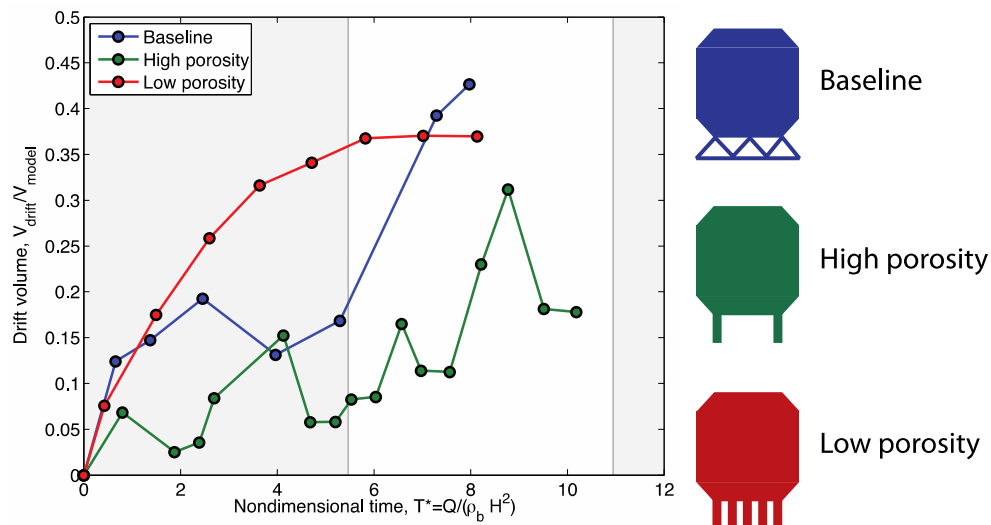


Figure 7. Total accumulated drift deposited around the simulated MAPO building configurations evaluated. The alternate gray and white shading indicates an elapsed time of about 1 year in the field ($T^* = 5.5$).

However, the results in Figure 7 only tell a small part of the story. In addition to affecting drift volume, the porosity of the substructure had profound effects on whether drifts formed predominately upwind or downwind of the structure. In the following section, we look in detail at the partitioning of the total drift volume in detail.

4.3 Upwind drift development

In Figure 8, we compare the upwind drift development observed for all three cases. For the baseline and high porosity cases, the drift evolutions tracked each other closely for the range of times tested, with the initial rate holding relatively steady until $T^* = 6$, at which point the growth rate quickly increased until reaching a maximum volume at $T^* = 8$. The low porosity case exhibited a similar trend, showing a slow initial accumulation followed by more rapid drift development, reaching a maximum value near $T^* = 8$. This initial slow development of the upwind drift seen in these results is consistent with what was observed for the A-S wind tunnel results, and appears to be a result of model distortion. This model distortion affects the initial stages of the upwind drift formation independent of porosity.

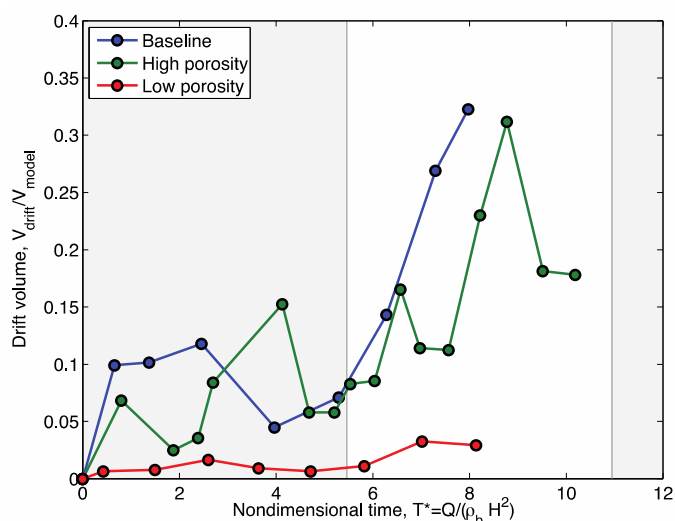


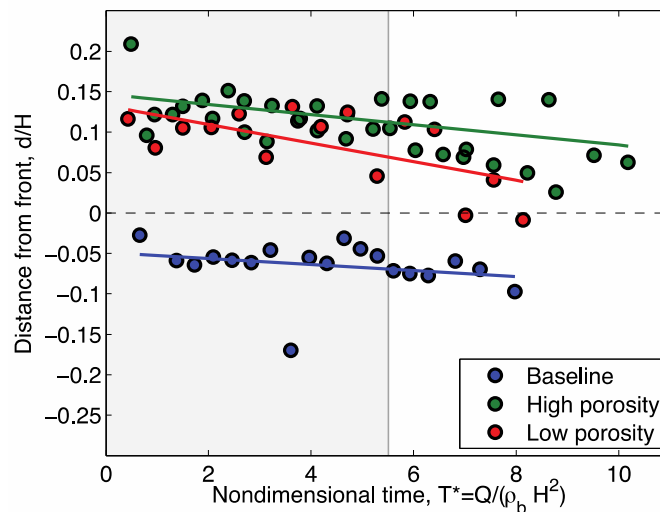
Figure 8. Upwind drift development as a function of elevated platform configuration.

The development of the drift for both the baseline and high porosity case proceeded in an oscillatory fashion (Fig. 8), with the accumulated drift volume sometimes increasing rapidly, and at other times decreasing rapidly; this oscillatory behavior is more pronounced for the high porosity case. This response seems to be an artifact of the wind tunnel modeling and is inconsistent with what is observed in the field where the drift grows monotonically in size until reaching an equilibrium state. The cause of this oscillatory behavior is not fully understood. Yet, the overall trend for the wind tunnel model was that of increasing drift volume with time and is consistent with field observations.

Also of note, the low porosity upwind volumes are an order of magnitude lower than the baseline and high porosity configurations. This behavior runs counter to our expectation that the higher porosity cases would generate smaller upwind drifts. Our rationale for this was that an open structure would result in less fluid momentum loss, promoting particle transport through the building substructure. On the other hand, a low porosity substructure would cause greater flow deceleration, encouraging particle deposition upwind of the building. To understand these counter-intuitive observations, in Section 5 we will take a closer look at the characteristics of the flow field that may be contributing to this unexpected behavior.

4.4 Drift encroachment

In addition to the drift size, it is also of value to understand how close the drift gets to the building. This “encroachment” of the drift on the structure can be a serious issue that not only will shorten a building’s service life, but can also compromise personnel safety, e.g., by blocking access points.



| Case description | Encroachment rate [d/HT*] |
|------------------|---------------------------|
| Baseline | 3.5×10^{-3} |
| High porosity | 7.9×10^{-3} |
| Low porosity | 1.2×10^{-2} |

Figure 9. Drift encroachment on the upwind side of the building.

The rate at which the drift approached the upwind side of the building was similar between the baseline and high porosity cases, yet, for the baseline

case, the upwind drift began immediately to form underneath the building. In the high porosity case, with only the four support legs, the drift did not reach the front of the building for the time range considered. This immediate accumulation of particles underneath the building can be attributed to span-wise cross members that lie perpendicular to the flow. These cross members protruded from the floor into the flow and were a surface feature that promoted particle deposition (i.e., a small scale trap) and drift initiation at that point. However, the cross members did not appear to affect the *rate* of drift encroachment but rather they provided a nucleation site for the upwind drift allowing the drift to form closer to the building. Although these span-wise members seemed to have a profound effect on the drift formation in the wind tunnel, they may have less of an effect in the field, depending on whether the 6-in. (15.2-cm) beams are placed on grade or buried during construction.

The results for the low porosity model also showed that the encroachment rate *did* appear to depend on support structure porosity. The low porosity case initially approached the front of the station at the same rate as the high porosity configuration, but then began to approach the building at a faster rate after $T^* = 4$, until the toe began to extend under the building at $T^* \approx 7$.

What these findings suggest for building life span is that designing the building substructure to promote initial drift formation as far as possible from the building would help increase the life of the building. Furthermore, higher substructure porosity reduced the rate of drift encroachment. Based on the results obtained in this study, the high porosity case considered may form a drift that will not reach the front of the building for an additional 2 years ($\Delta T^* = 12$) in comparison to the low porosity case. Furthermore, in comparison to the baseline case presented here, the upwind drift for the high porosity geometry would not reach the building for about 3.5 years ($T^* = 19$), while for the baseline case, the drift immediately forms under the building.

4.5 Downwind drift development

In contrast to the upwind drift development, this study showed that the growth rate of the downwind drift increased with decreasing substructure porosity. The low porosity case, where the supporting structure was a dense array of posts that significantly limited flow underneath the building, had the highest growth rate and equilibrium volume for the downwind

drift (Fig. 10). The baseline configuration, with a trusswork substructure, reached an equilibrium volume that was only one third of the equilibrium volume for the low porosity case. The highest porosity case, with a substructure consisting of four posts at each corner of the building, did not develop a downwind drift at all. This inverse relationship between porosity and downwind drift volume can be partially explained by the higher fluid momentum losses as the substructure porosity decreases. The momentum loss under the building results in lower flow velocities behind the building, which translates into larger downwind drifts. From these results, it appears that an equilibrium downwind drift takes about 1 year to develop.

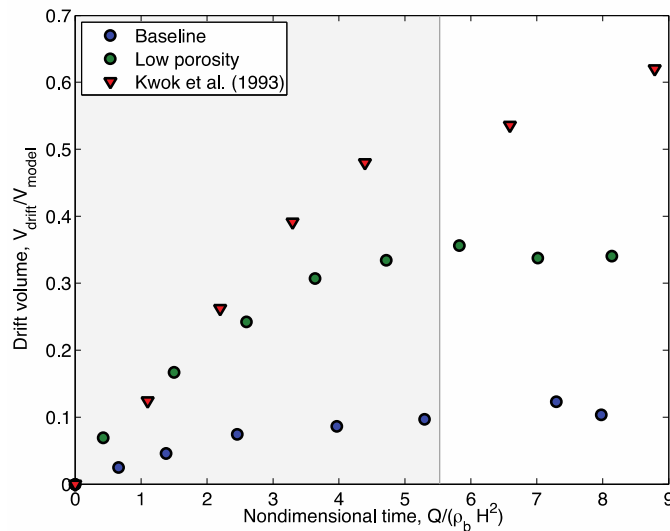


Figure 10. Comparison of downwind drift volumes with experiment done by Kwok et al. (1993). (Note—high porosity model did not develop a downwind drift.)

For comparison, we also included the data of Kwok et al. (1993) in Figure 10. They also studied drifting around an elevated building. Their tests closely resembled the geometry of the MAPO building with respect to the orientation to the wind, aspect ratios of building length : width : height, and the spacing between the building and ground. Furthermore, the substructure geometry used by Kwok et al. (1993) was identical to the high porosity case studied here (one post on each corner). However, the results obtained by Kwok et al. (1993) more closely match the results we obtained for our *low* porosity case, where they observed no upwind drift in their model studies and the size and development rate of the downwind drift more closely matched those measured for our low porosity case, as shown in Figure 10.

Resolution of this discrepancy required a close look at the few key differences between the Kwok et al. (1993) case and our seemingly identical case. First, the scale of the model used in their study was about 1:140, while the scale of the MAPO building in this study was 1:30. Furthermore, the material used to simulate snow by Kwok et al. (1993) was sodium bicarbonate, while we used glass beads. These two factors, taken together, help to explain the difference in performance between the two studies, as well as further our understanding of porosity effects on drift formation.

Consider the model scale effects. The model scale of the Kwok et al. (1993) experiments was about 4.7 times smaller than ours, resulting in much smaller physical clearance height between the bottom of the model and the ground (or bottom gap height, h) (1.8 cm versus 8.5 cm for our experiments). This in and of itself constricted that flow somewhat, by reducing the “pore” area by over an order of magnitude. Thus, the Kwok et al. (1993) case had a somewhat more restricted flow simply because of the smaller scale.

Furthermore, the scale effect played a second role. The concentration, C , of the aerosolized particles decreases with elevation, z , approximately according to Mellor (1965):

$$\frac{C(z)}{C_a} = \left(\frac{a}{z}\right)^{-\frac{w_f}{u_*}} \quad (7)$$

where C_a is a reference concentration at a reference height, a . The terminal particle fall velocity and friction velocity associated with the boundary layer flow¹ is denoted by w_f and u_* , respectively. This expression indicates that the concentration is very high near the ground and falls off exponentially with elevation. Thus, with a small bottom gap, on average a higher concentration of particulate flow is being carried in the narrow space than would be transported through a taller opening.

¹ The friction velocity is related to the near bed velocity profile by a law-of-the-wall expression such as (Prandtl-von Karman equation)

$$\frac{U(z)}{u_*} = \frac{1}{\kappa} \ln\left(\frac{z}{z_0}\right)$$

where U is the velocity at elevation, z , z_0 is the aerodynamic roughness height of the rough ground surface, and $\kappa \approx 0.4$ is von Karman's constant.

This effect is illustrated by comparing the estimated variation of particulate concentration carried by the flow that was passing under the building as we have done in Figure 11. In this plot we normalized the elevation of all of the drift concentration data by the height of the bottom gap, such that $z/h = 1$ corresponded to the bottom of the elevated building.

First, we show data measured in the field (symbols) and published in Mellor (1965) for drifting snow concentrations for elevations that correspond to the prototype scale. This is compared to the computed snow concentration (black line) using eq (7). This shows that the concentration estimated using eq (7) does a reasonable job of representing observed conditions.

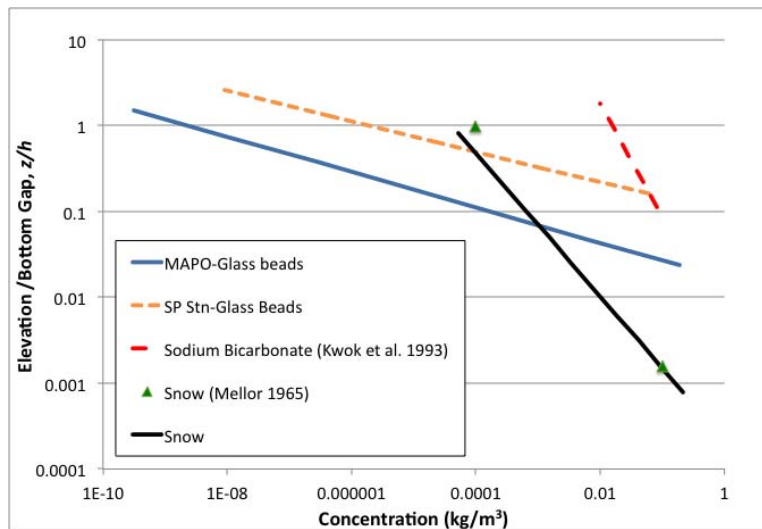


Figure 11. Comparison of the concentration of particles carried by the wind between the field condition and that estimated for the model cases. A normalized elevation, $z/h = 1$ corresponds to the bottom of the elevated building.

The remaining curves shown in Figure 11 are the estimated concentration profiles for the test conditions published by Kwok et al. (1993) and for this study. This shows that, based on the model scale used by Kwok et al. (1993) and using the particle properties for their snow simulant (sodium bicarbonate), the aerosol concentration is 3–4 orders of magnitude higher than the observed concentrations in the field. This increased bedload transport takes momentum from the flow in a similar manner to reduction of the porosity under the building, with the net result also being very similar, i.e., the trends in drift formation for the low porosity case in this study being very similar to that obtained by Kwok et al. (1993) for a seemingly high porosity case.

Also, for comparison, we show the drift concentration with height for the simulations conducted in this study. This tells us that the model concentrations for the A-S station were closer in line with that observed in the field, while for the MAPO building the concentrations tended to be lower than field observations. Though it is difficult to get an exact similitude between reduced scale model and prototype conditions—because of model distortions such as discussed in section 2—the drift concentrations in this study were close to the near bed concentrations observed in the field.

From this study we identified several significant findings. First, the point at which a drift starts did not only depend on larger scale features of the flow, such as separation zones, but also seemed to depend on smaller scale features that one might not expect to have a pronounced influence on drift formation. For the MAPO building studied here, we found that the spanwise cross members on the baseline support structure served as a nucleation point for drift formation that caused the drift to start much closer to the building than it would if the ground were clear of such obstructions. Based on these findings, one needs to carefully consider what is placed under an elevated building, and where it is placed during the design, construction, and operation phases, to properly manage drift formation around the buildings and prolong the usable building life.

We noted that in this wind tunnel study we did not consider the effects of the background snow accumulation (~24 cm annually) on drift evolution and encroachment on the buildings. This is difficult to simulate in the wind tunnel, as it requires adding this accumulation uniformly around the model while the drift is evolving. From our results, it appears that differences in the rate of drift accumulation attributable to porosity effects may prolong the life of a building by 2–3 years; over that time the background accumulation would be 50–75 cm or about 30% of the height (2.5 m) of the substructure. Based on this, the clearance between the bottom of the building and the snow surface may further choke the flow, reducing effectiveness of the higher porosity substructure. Thus, we consider the time estimates for prolonging the life of the building obtained here as a reasonable upper limit to what can be hoped for through careful control of the substructure porosity.

Another finding from this study was that, in addition to changing the total drift volume deposited around the building, substructure porosity also affects how the drift is distributed, either mostly upwind of the building (as

in the case of high porosity) or mostly downwind of the building (low porosity case) or a partitioning of the drift between both locations. Such trends, though not entirely unexpected, were counter-intuitive in that one expects that blocking of flow caused by the low porosity structure would deposit a drift upwind of the structure, while an open substructure design would allow more drifting snow to be carried downstream of the building where it would be deposited in the wake behind the structure. To resolve this seeming paradox, we endeavored to better understand the changes in the flow structure around the building imposed by the changing substructure porosity and how that may relate to the drift deposition. This analysis is the focus of the next section.

5 Computational experiments

5.1 Approach

We conducted computation fluid dynamics (CFD) calculations to shed light on how the flow around the elevated building responded to variation in the porosity under the building. The calculations were done using a compressible, turbulent flow solver. This is part of the OpenFOAM (SGI Corporation, Fremont, CA) suite of solvers, which includes the capability to adjust permeability, which is related to porosity, in specified regions. Using permeability as an analog for the substructure blockage, rather than explicitly modeling the detailed substructure geometry, was more computationally efficient—yielding faster solution times—and allowed us to generalize the trends over a range of structures that have varying degrees of substructure blockage.

The CFD solver employed here also allows the user to specify the oncoming flow's turbulence characteristics and the wall (bed) roughness height; these parameters were kept constant for this set of numerical experiments.

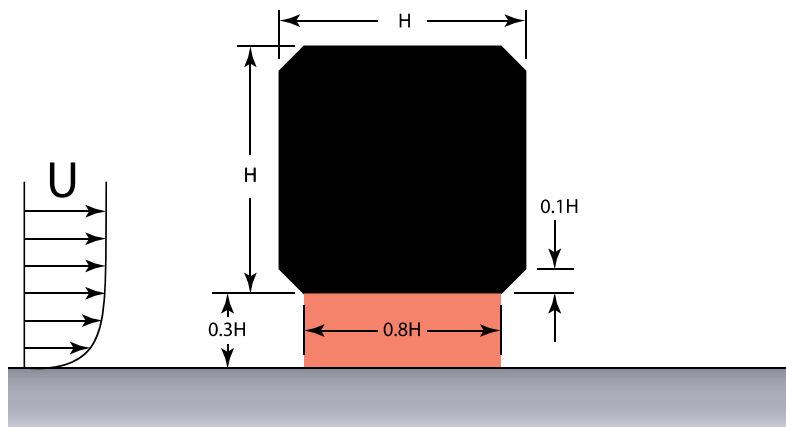


Figure 12. Schematic of CFD configuration. For comparison of the dependence of the flow field on the substructure porosity, the permeability of the red shaded region was varied from $\kappa = 1$ to $2 \times 10^{-6} \text{ m}^2$.

Permeability was determined as follows. The volumetric flow rate, Q (m^3/s), through a porous medium is related to the pressure gradient $\Delta p/\Delta x$ across the medium. When Q is linearly related to the pressure gradient, the flow can be described by Darcy's Law, given as

$$Q = \frac{\kappa \Delta p A}{\mu \Delta x} \quad (8)$$

and the constant of proportionality κ (m^2) is the permeability for a constant cross-sectional area, A (m^2), medium length, Δx (m), and fluid dynamic viscosity, μ ($\text{Pa}\cdot\text{s}$). The permeability can be loosely interpreted as the average pore area for conveying the flow through the porous media. Therefore, we can vary the permeability in the region between the building and the ground (shown as the red shaded region in Fig. 12) and use this parameter as an analog for changes in the substructure clutter that “chokes” the flow between the building and the floor.

To determine the permeability range to consider, a CFD model was constructed with the low porosity substructure used in this study placed in a rectangular duct. The pressure drop across the substructure could be calculated from the flow solution, and the permeability was computed directly using eq (8). From this we determined the permeability for the low porosity substructure to be $2 \times 10^{-6} \text{ m}^2$. The permeability for the high porosity case was estimated based on the flow area for the high porosity case. The approximate permeability was about 10^{-2} m^2 . Our best estimate was that the baseline case is less than this, but in the range $10^{-2} \geq \kappa \geq 10^{-4} \text{ m}^2$.

For the geometry shown in Figure 12, we ran four CFD simulations with $1 \geq \kappa \geq 2 \times 10^{-6} \text{ m}^2$, with discrete values being 1, 10^{-4} , 10^{-5} , and $2 \times 10^{-6} \text{ m}^2$. Thus, the range of permeability tested using the CFD simulations encompassed the range of permeabilities for the substructures explored in the wind tunnel experiments.

5.2 Results

The structure of the flow around an elevated building dictates drift evolution and in some measure can be altered by the porosity of the building support structures. Particles (snow in the field, and glass beads in the wind tunnel) will begin to deposit in regions where the wall shear stress, defined as $\tau = \mu \nabla u$, is below the level necessary to initiate or maintain particle motion (known as the critical shear stress, τ_c). The magnitudes of the wall shear stress for values of permeability from $1 \geq \kappa \geq 2 \times 10^{-6} \text{ m}^2$ are plotted in Figure 13. We looked for regions where the wall shear stress fell below the critical value; these regions are indicated by the darker blue regions bordered by a white contour in Figure 13, and are identified as locations where drifts will most likely would begin to accumulate.

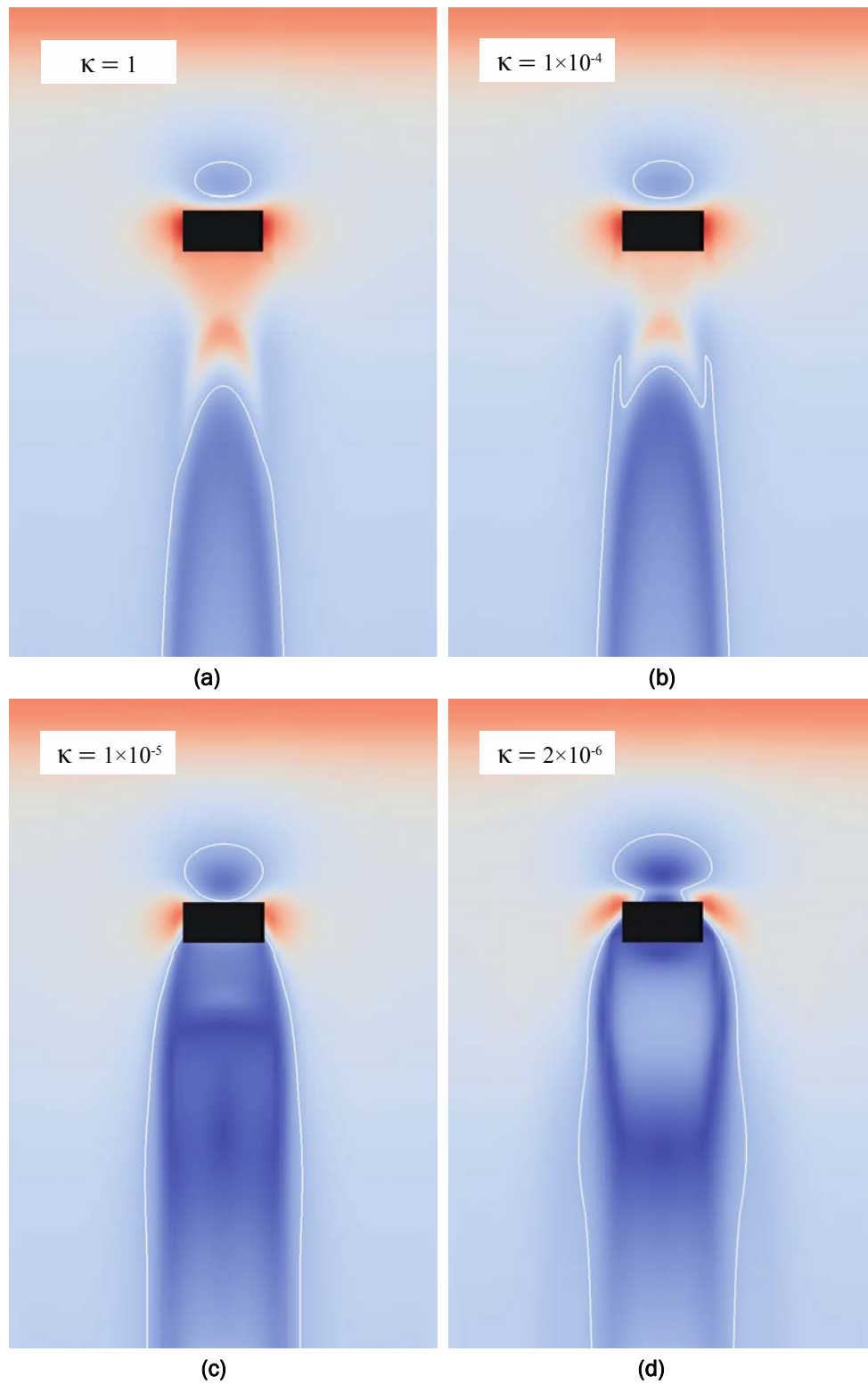


Figure 13. Wall shear stress magnitude. High and low values of wall shear stress are indicated by regions of red and blue, respectively. Darker blue regions enclosed by a white contour are areas where the wall shear stress is below the critical value needed for particle motion.

As mentioned previously, the lowest value of permeability that we tested, $\kappa = 2 \times 10^{-6} \text{ m}^2$, corresponds closely to the low porosity wind tunnel configuration. For this case, the upwind and downwind subcritical regions continued to grow to the point where now both regions were wider than the building. In the downwind subcritical region, the areas of particularly low shear stress were now more localized to “filaments” extending from the sides of the building to a patch located approximately four building lengths downstream.

The main aim of the numerical experiments was to identify the flow mechanisms leading to the unexpected drift behavior observed in the wind tunnel experiments, where the upwind drift size increased with increasing substructure porosity, and the downwind drift size increased with decreasing substructure porosity. As discussed previously, we would expect particles to accumulate in regions where the wall shear stress was lower than the critical stress value. As the substructure porosity decreased, we observed a growth in the upwind subcritical region’s area and a decrease in the minimum shear stress observed within the region due to the deceleration of the oncoming flow by the substructure clutter. However, for the lowest porosity wind tunnel configuration, which corresponds to the $\kappa = 2 \times 10^{-6} \text{ m}^2$ CFD calculation, this increase in the upwind subcritical region’s area did not result in a higher upwind drift growth rate. In fact, we observed a markedly lower growth rate than the high porosity configurations, even though the calculated wall shear stress field (Fig. 13d) indicated that an upwind drift would likely form in this location and the lower values of shear stress within the subcritical region suggest that the growth rate should be higher with respect to the high porosity configurations. Yet, the velocity fields shown in Figure 14 may be telling us a different story.

In Figure 14, we plot the centerline velocity magnitude for each of the 4 CFD cases studied. For the lowest permeability ($\kappa = 2 \times 10^{-6} \text{ m}^2$), the plot of the centerline velocity magnitude (Fig. 14d) showed a small upwind separation bubble at the floor, i.e., a region of slow, recirculating fluid (indicated by the near-floor region of blue just upwind of the building). This flow structure would function in similar fashion to a solid bump on the floor and deflect the oncoming particle-laden flow over this region of subcritical wall shear stress, thus preventing particles from depositing and suppressing drift deposition upwind of the building. Instead of being deposited upwind of the building, the particles would continue to travel through the

building substructure and eventually settle in the low shear stress envelope that starts immediately behind the building.

This counter-intuitive result tells us that a less porous substructure configuration may be more effective (but only for very special flow conditions) in preventing upwind drift accumulation than one that is completely free of flow impediments. However, further investigation would be needed to put these findings into practice.

This CFD analysis was useful to help understand how the building substructure can affect the flow field. However, these simulations only characterize a flow field at the early stages where the drift has either not yet begun to form or is so small that it does not have significant influence on the flow structure. CFD methods can further benefit our understanding by adding drift development to the flow simulations. Providing a robust capability for predicting drift initiation and evolution in CFD solvers remains as a future work.

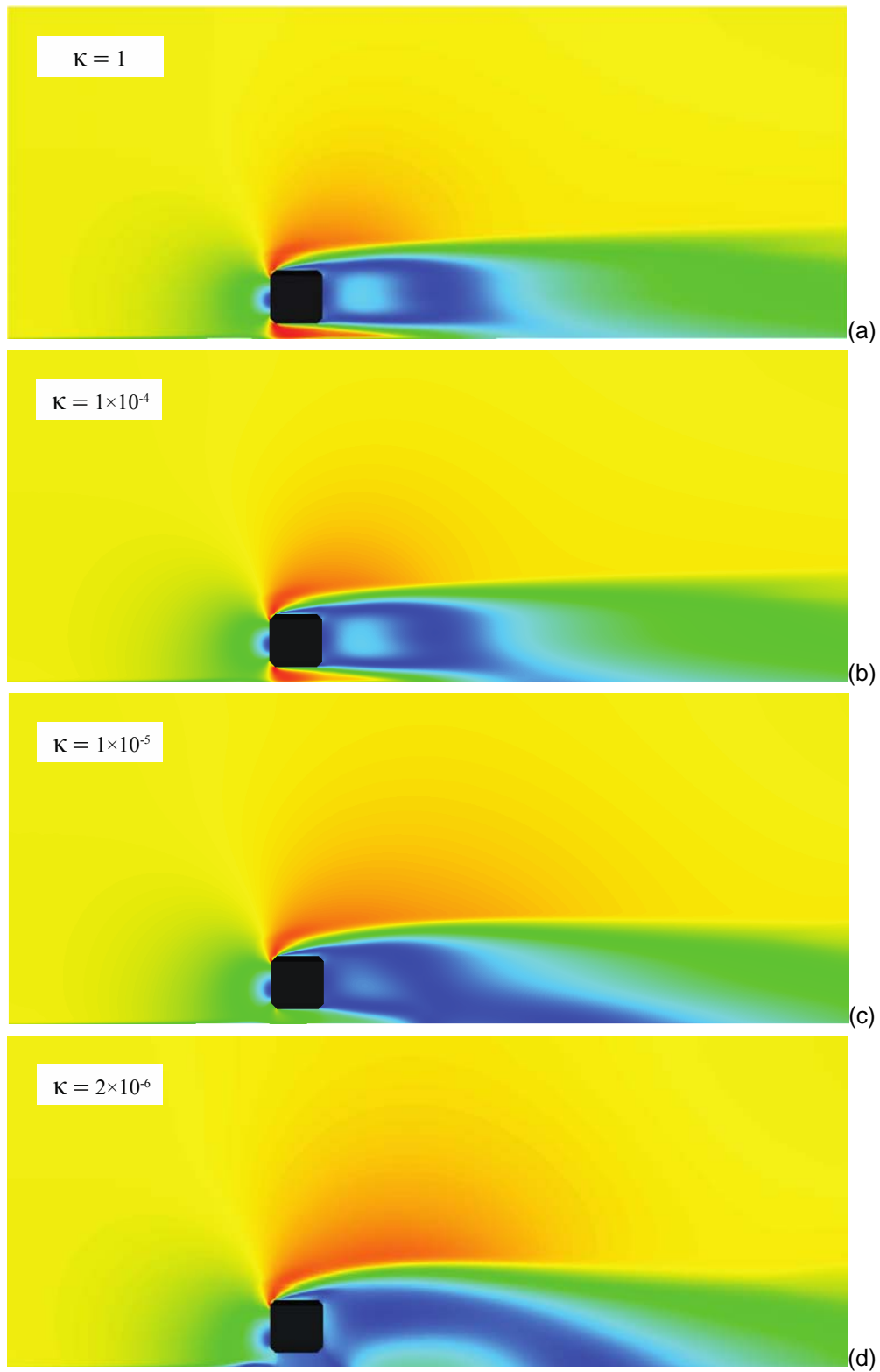


Figure 14. Building centerline velocity magnitude fields. Red indicated a high velocity and blue indicates low velocity.

6 Concluding remarks

We performed wind tunnel measurements and complementary CFD calculations to study the effects of substructure clutter on drift development near elevated buildings. The volume scaling of Lever and Haehnel (1995) was tested using field data for the elevated Amundsen-Scott Station at the South Pole and comparable wind tunnel experiments. The field and laboratory drift behaviors were shown to be in relatively good agreement, therefore validating this approach for using a scaled mass transport as a proxy for time in field and wind tunnel data correlations.

We then conducted drifting experiments for a prototypical Antarctic building (a rectangular prism with chamfered edges that has the same proportions as the MAPO building) with three support structure configurations that have varying porosity (and permeability) to explore the effects of substructure clutter on snow drift evolution. The three cases were 1) a baseline case that has the support structure used in the field for the MAPO building, 2) a high porosity case supported by four columns, one at each corner of the building, and 3) a low porosity case with substructure consisting of a matrix of closely spaced support posts.

6.1 Significant findings

1. The total drift volume accumulated around the structure was reduced as porosity was increased from the baseline case to the highest porosity case (building supported by four columns, $\kappa \approx 10^{-2} \text{ m}^2$). However, reducing the porosity from the baseline case did not produce a significant change in the *total* accumulated drift volume.
2. The upwind drift accumulation rate increased with increasing porosity. The upwind drift was practically nonexistent for the low porosity case studied ($\kappa = 2 \times 10^{-6} \text{ m}^2$).
3. The downwind drift growth rate decreased with increasing porosity, with no downwind drift observed for the minimal support configuration (only one post at each corner of the building), which was likely a result of higher particle momentums (for higher substructure porosity) as the flow exited the space under the elevated building. For the low porosity case, the downwind drift was the dominant feature with only a very small upwind drift forming.

4. Some features under the building or as part of the support structure can promote drift initiation close to the building and cause the drift to rapidly encroach on the building. This is a potentially dangerous drifting behavior that may also lead to shorter building service life spans. In this study, span-wise cross members on the baseline support structure for the MAPO building served as nucleation points for drift formation that promoted the drift to form much closer to the building than occurs when these features were not present. Careful thought during the design phase needs to be given to avoiding such structural features that negatively affect drift control.
5. Based on the observed drift encroachment rates (rate at which the upwind drift approaches the front of the building during drift evolution) measured in the wind tunnel, it may be possible to prolong the life of these buildings by 2 or more years by increasing substructure porosity and careful design and construction of the substructure.

To better understand the trends in the wind tunnel results, we used Computational Fluid Dynamics (CFD) to take a closer look at the flow field surrounding the buildings. We used substructure permeability, κ (m^2), as an analog for substructure clutter to allow us to efficiently evaluate the trends associated with changes in substructure porosity. This was done, rather than simulating the detailed geometry of each case evaluated in the wind tunnel, as it is more computationally efficient, and provided general trends that were independent of specific substructure geometry. These simulations did not address the presence or location of specific sub-building features, such as trusses, conduits, stairways, etc. To determine the effect of such specific features would require a more detailed numerical study that simulates the flow through a proposed support structure design, which we leave for proposed future work.

To evaluate the trends of flow field surrounding the buildings as a function of substructure blockage, we ran four simulations with substructure permeability ranging from $\kappa = 1$ to $2 \times 10^{-6} \text{ m}^2$, which encompassed the range of permeabilities for the substructures we studied. Using the results of the CFD simulations, we computed the shear stress at the ground to determine the regions where it was likely that drifts would start to form. From this, we found that, for all of the cases studied, there were regions both upstream and downstream of the buildings where the shear stress was below the critical value for particle motion; therefore, these would be potential locations for drifts to start to form. However, the size and proximity of

these subcritical regions to the building changed greatly with substructure permeability.

We also observed that, for permeabilities in the range of the high porosity and baseline substructures, a strong Venturi effect was visible under the building, which elevated the velocity under the building. This seemed to have the effect of sweeping the area clean under the building and ejecting particles out from under the building with enough momentum that they did not form a large a drift behind the building.

The velocity was not elevated under the building for the case where the porosity (and permeability) was low. This seemed to allow the particles to deposit more readily in the region immediately behind the building. In addition, for the low porosity case, we observed the formation of a flow separation bubble where we would expect the upwind drift to form. We hypothesize that this flow structure may suppress drift formation by deflecting particle-laden flow up and over this separation bubble. However, more work is needed to understand the details of this phenomenon, and whether it could be used as an alternative approach to controlling the development of an upwind drift.

6.2 Suggestions for future work

6.2.1 Continuation of the numerical snowdrift deposition model development

The CFD simulations that were conducted as part of this study looked only at the effect that the building had on the flow, uncoupled from the snow dynamics. We propose expanding this model to include drift evolution and the feedback on the flow field that the evolving drift creates. We will use, as initial test cases, the field survey data of the drifts around the Amundsen-Scott Station and compare the numerical results to the field data for these buildings.

6.2.2 Control of drifting snow on garage shop entrance

The use of passive and active methods to mitigate snowdrift formation in front of the entrance to the garage shop (entrance to the arches) will be studied. A scale model of the terrain and buildings around and over the arches, including the Amundsen-Scott South Pole Station, will be built and tested in the CRREL Environmental Wind Tunnel. We will initially use

this model to reproduce the baseline drift formation observed at season opening in 2009. Then the model will be used to explore flow diverters, drift management strategies, and other methods to prevent deposition of snow in the garage entrance area. From this task we will provide guidance on how to prevent drift deposits in the garage entrance area.

References

- Anno, Y. 1984. Requirements for modeling of a snowdrift, *Cold regions science and technology* **8**: 241–252.
- Budd, W. F., W. R. J. Dingle, and U. Radok. 1966. The Byrd snow drift project: outline and basic results. *Studies in Antarctic Meteorology* **9**: 71–134.
- Kim, D. H., K. C. S. Kwok, and H. F. Rohde. 1990. in *Proceedings of the First Pacific/Asia Offshore Mechanics Symposium, The International Society of Offshore and Polar Engineers, Seoul, Korea*, pp. 45–50.
- Kwok, K. C. S., D. J. Smedley, and D. H. Kim. 1993. Snowdrift around Antarctic buildings—Effects of corner geometry and wind incidence. *International Journal of Offshore and Polar Engineering* **3**: 61–65.
- Lever, J. H., and R. H. Haehnel. 1995. Scaling snowdrift development rate. *Hydrological Processes* **9**: 935–946.
- Mellor, M. 1965. *Cold Regions Science and Engineering, Part III, Section A3c: Blowing Snow*. U.S. Army Cold Regions Research and Engineering Laboratory. Monograph series.
- Mosley-Thompson, E., J. F. Paskievitch, A. J. Gow, and L. G. Thompson. 1999. Late 20th century increase in South Pole snow accumulation. *Journal of Geophysical Research* **104**: 3877–3886.
- Skoog, K. 2009. *Summarized Drift Data FY09 Final Draft*.
- Tabler, R. D. 1991. in *Sixth International Cold Regions Engineering Conference, West Lebanon, NH, USA, 26–28 February 1991*, pp. 729–738.
- Thom, A. 1943. *Blockage Corrections in a Closed High-speed Tunnel*. His Majesty's Stationery Office.

REPORT DOCUMENTATION PAGE

Form Approved
OMB No. 0704-0188

Public reporting burden for this collection of information is estimated to average 1 hour per response, including the time for reviewing instructions, searching existing data sources, gathering and maintaining the data needed, and completing and reviewing this collection of information. Send comments regarding this burden estimate or any other aspect of this collection of information, including suggestions for reducing this burden to Department of Defense, Washington Headquarters Services, Directorate for Information Operations and Reports (0704-0188), 1215 Jefferson Davis Highway, Suite 1204, Arlington, VA 22202-4302. Respondents should be aware that notwithstanding any other provision of law, no person shall be subject to any penalty for failing to comply with a collection of information if it does not display a currently valid OMB control number. **PLEASE DO NOT RETURN YOUR FORM TO THE ABOVE ADDRESS.**

| | | | | | |
|---|--------------------|---|-----------------------------------|---|--|
| 1. REPORT DATE (DD-MM-YYYY) September 2012 | | 2. REPORT TYPE Final | | 3. DATES COVERED (From - To) | |
| 4. TITLE AND SUBTITLE Effects of Support Structure Porosity on the Drift Accumulation Surrounding an Elevated Building | | | | 5a. CONTRACT NUMBER | |
| | | | | 5b. GRANT NUMBER | |
| | | | | 5c. PROGRAM ELEMENT NUMBER | |
| 6. AUTHOR(S) Arnold Song and Robert Haehnel | | | | 5d. PROJECT NUMBER | |
| | | | | 5e. TASK NUMBER | |
| | | | | 5f. WORK UNIT NUMBER | |
| 7. PERFORMING ORGANIZATION NAME(S) AND ADDRESS(ES) U.S. Army Engineer Research and Development Center Cold regions Research and Engineering Laboratory U.S. Army Engineer Research and Development Center 72 Lyme Road Hanover, NH 03755 | | | | 8. PERFORMING ORGANIZATION REPORT NUMBER ERDC/CRREL TR-12-7 | |
| 9. SPONSORING / MONITORING AGENCY NAME(S) AND ADDRESS(ES) National Science Foundation Office of Polar Programs, AIL Arlington, VA | | | | 10. SPONSOR/MONITOR'S ACRONYM(S) | |
| | | | | 11. SPONSOR/MONITOR'S REPORT NUMBER(S) | |
| 12. DISTRIBUTION / AVAILABILITY STATEMENT Approved for public release; distribution is unlimited. | | | | | |
| 13. SUPPLEMENTARY NOTES | | | | | |
| 14. ABSTRACT This study focuses on the effects of elevated building substructure porosity on the accumulation of drifting snow. We conducted wind tunnel experiments of the snowdrift accumulation and numerical simulations to determine the flow field around a prototypical elevated building (based on the Martin A. Pomerantz Observatory or MAPO) with varying substructure porosity. We found that the total drift volume accumulated decreases as the substructure porosity increases (i.e., the substructure has less clutter). Furthermore, substructure porosity influenced the proportion of the drift deposited upwind or downwind of the structure, with a more porous substructure depositing most of the drift upwind of the structure; for low substructure porosity, most of the drift is deposited in the lee of the structure. Numerical simulations revealed that, for low substructure porosity a separation bubble can form upwind of the building that appears to direct particles over the upwind region of subcritical shear stress and suppress formation of the upwind snowdrift. Porosity and the presence of ground-based clutter also affected the rate of drift encroachment. The results of this study suggest that applying care in the design of the substructure could prolong the life of a building by 2 or more years. | | | | | |
| 15. SUBJECT TERMS Drift accumulation Elevated building | | Elevated building substructure porosity Mathematical modeling Physical modeling | | Snow drifting Wind tunnel experiments | |
| 16. SECURITY CLASSIFICATION OF: | | | 17. LIMITATION OF ABSTRACT | 18. NUMBER OF PAGES | 19a. NAME OF RESPONSIBLE PERSON |
| a. REPORT | b. ABSTRACT | c. THIS PAGE | | | 19b. TELEPHONE NUMBER (include area code) |
| U | U | U | None | 44 | |